

lessen encodes a zebrafish *trap100* required for enteric nervous system development

Jacy Pietsch¹, Jean-Marie Delalande¹, Brett Jakaitis¹, James D. Stensby¹, Sarah Dohle¹, William S. Talbot², David W. Raible³ and Iain T. Shepherd^{1,*}

The zebrafish enteric nervous system (ENS), like those of all other vertebrate species, is principally derived from the vagal neural crest. The developmental controls that govern the specification and patterning of the ENS are not well understood. To identify genes required for the formation of the vertebrate ENS, we performed a genetic screen in zebrafish. We isolated the *lessen* (*lsn*) mutation that has a significant reduction in the number of ENS neurons as well as defects in other cranial neural crest derived structures. We show that the *lsn* gene encodes a zebrafish orthologue of *Trap100*, one of the subunits of the TRAP/mediator transcriptional regulation complex. A point mutation in *trap100* causes a premature stop codon that truncates the protein, causing a loss of function. Antisense-mediated knockdown of *trap100* causes an identical phenotype to *lsn*. During development *trap100* is expressed in a dynamic tissue-specific expression pattern consistent with its function in ENS and jaw cartilage development. Analysis of neural crest markers revealed that the initial specification and migration of the neural crest is unaffected in *lsn* mutants. Phosphohistone H3 immunocytochemistry revealed that there is a significant reduction in proliferation of ENS precursors in *lsn* mutants. Using cell transplantation studies, we demonstrate that *lsn/trap100* acts cell autonomously in the pharyngeal mesendoderm and influences the development of neural crest derived cartilages secondarily. Furthermore, we show that endoderm is essential for ENS development. These studies demonstrate that *lsn/trap100* is not required for initial steps of cranial neural crest development and migration, but is essential for later proliferation of ENS precursors in the intestine.

KEY WORDS: Neural crest, Zebrafish, Craniofacial, ENS development, *lessen* (*lsn*), *trap100* (*thrap4*), Proliferation

INTRODUCTION

The enteric nervous system (ENS) is derived from multipotent precursor cells that migrate from the neural crest to the intestine (Furness, 1987; Gershon, 1994). In all vertebrate species studied, the majority of the ENS is derived from neural crest cells that migrate from the vagal region (Newgreen and Young, 2002b). As the ENS precursors migrate, they proliferate and differentiate to form a wide variety of neuronal subtypes (Furness, 1987; Gershon, 1994). Molecules in the environment as well as lineage restrictions within the ENS precursors determine the number and specific cell fates acquired by these precursors. Failure of ENS precursors to colonize the complete gut results in the absence of enteric ganglia along varying lengths of the colon (colonic aganglionosis) (Newgreen and Young, 2002a; Newgreen and Young, 2002b). This is the most common cause of congenital intestinal obstruction in humans and is clinically referred to as Hirschsprung's disease (HSCR) (Kapur, 1999b; Newgreen and Young, 2002a).

The molecular mechanisms that control the specification and proliferation of the neural crest have been studied extensively. Several secreted signalling molecules and their associated receptors have been identified that control directly and indirectly the morphogenesis of the ENS. These include GDNF (Cacalano et al., 1998; Enomoto et al., 1998; Moore et al., 1996; Pichel et al., 1996; Schuchardt et al., 1994), neurturin (Heuckeroth et al., 1999; Heuckeroth et al., 1998; Rossi et al., 1999), endothelin

3 (Baynash et al., 1994; Hosoda et al., 1994; Yanagisawa et al., 1998), BMP2/4 (Chalazonitis et al., 2004; Wu and Howard, 2002), Ihh (Indian hedgehog) (Ramalho-Santos et al., 2000), Shh (sonic hedgehog) (Fu et al., 2004; Ramalho-Santos et al., 2000; Sukegawa et al., 2000), NT3 (Chalazonitis et al., 2001; Chalazonitis et al., 1994) and CNTF (Chalazonitis et al., 1998).

In addition to these signalling molecules, a number of transcription factors have been implicated as having a role in the specification of the ENS including Mash1 (Guillemot et al., 1993), Phox2b (Pattyn et al., 1999), SOX10 (Herbarth et al., 1998; Kapur, 1999a; Pattyn et al., 1999; Southard Smith et al., 1998), Hox1111 (Hatano et al., 1997; Shirasawa et al., 1997), Hoxb5 (Kuratani and Wall, 1992; Pitera et al., 1999), Hand2 (Cserjesi et al., 1995; Howard et al., 1999; Srivastava et al., 1995; Wu and Howard, 2002) and AP2 α (Barralogo-Gimeno et al., 2004; Knight et al., 2003; O'Brien et al., 2004). Perturbation of the function of these signalling molecules and transcription factors leads to defects in ENS. Furthermore, mutations in some of these genes have been identified in patients affected with HSCR (Amiel and Lyonnet, 2001; Puri et al., 1998); however, mutations in these known genes can only account for ~60% of familial HSCR (Amiel and Lyonnet, 2001; Puri et al., 1998).

Classical genetic studies of development have proven their utility in creating a molecular underpinning of the metazoan body plan, but the model organisms exploited to create that framework lack many of the organs found in vertebrates. To date, the genes identified as involved in ENS development have been identified indirectly. We therefore conducted a forward genetic screen in zebrafish to identify genes that when mutated would cause perturbations in the development of the ENS. One of the mutants we identified in this screen is *lessen* (*lsn*). Fish with a mutation in *lsn* have a significant reduction in the number of enteric neurons but also have defects in other neural crest and non-neural crest derived tissues, including the CNS and the intestine. We show that the *lsn* mutation disrupts a

¹Department of Biology, Emory University, Rollins Research Center, 1510 Clifton Road, Atlanta GA 30322, USA. ²Department of Developmental Biology, Stanford University School of Medicine, Stanford CA 94305, USA. ³Department of Biological Structure, University of Washington, Box 357420, Seattle WA 98195, USA.

*Author for correspondence (e-mail: ishephe@emory.edu)

zebrafish *trap100* (*thrap4* – Zebrafish Information Network) that is required for the proliferation of enteric precursors within the embryonic intestine. Furthermore, we also show that *trap100* is specifically required for the normal development of other cranial neural crest-derived structures, revealing that this gene has previously unappreciated tissue specific functions during embryogenesis. Transplantation of wild-type endoderm into *lsn/trap100* mutants induces posterior pharyngeal arch cartilage development, which indicates that *trap100* acts autonomously in the endoderm. Consequently this suggests that neural crest defects are secondary to endoderm defects in *lsn/trap100* mutants. This is consistent with our finding that the ENS fails to develop in zebrafish that lack intestinal endoderm.

MATERIALS AND METHODS

Zebrafish maintenance and breeding

Fish were raised and kept under standard laboratory conditions at 28.5°C (Westerfield, 1993). Embryos were staged and fixed at specific hours or days post fertilization (hpf or dpf), as described by Kimmel et al. (Kimmel et al., 1995). To better visualize internal structures in some experiments, embryos were incubated with 0.2 mM 1-phenyl-2-thiourea (Sigma) to inhibit pigment formation (Westerfield, 1993).

Immunocytochemistry

Embryos were processed for immunocytochemistry as previously described (Raible and Kruse, 2000). Differentiated enteric neurons and cranial ganglia neurons were revealed with the anti-Hu mAb 16A11 (Molecular Probes) that labels differentiated neurons (Marusich et al., 1994). Serotonergic neurons were identified with an anti-5HT rabbit polyclonal antisera (Immunostar). ENS precursors were revealed with an anti-Phox-2b rabbit polyclonal antisera (Pattyn et al., 1997). Proliferating cells were identified using an anti phosphohistone-H3 mAb clone (Ser10) (Upstate) (Ajiro et al., 1996). All mAbs were visualized using an Alexa Fluor 568 anti-mouse IgG antibody (Molecular Probes) or an Alexa Fluor 488 anti-mouse IgG antibody in double-label experiments (Molecular Probes). The rabbit polyclonal Ab was visualized using an Alexa Fluor 568 anti-rabbit IgG antibody (Molecular Probes).

Mutagenesis and screening

Males of the AB line treated with ENU as described previously bred with wild-type females for at least two generations, then in-crossed to derive recessive mutations to homozygosity (Haffter et al., 1996). Clutches of in-crossed 96 hpf embryos were fixed and processed for immunocytochemistry using anti Hu mAb 16A11. The number of enteric neurons was determined in a 10-somite segment of the intestine extending anteriorly from the end of the yolk extension as described previously (Shepherd et al., 2004).

Apoptosis assay

Apoptotic cell death was detected in whole embryos by terminal transferase dUTP nick-end labelling (TUNEL) (In situ Cell Death Detection Kit; POD; Roche) as described (Knight et al., 2003).

Cartilage staining and histological methods

Cartilages were stained with Alcian Blue as described (Schilling et al., 1996). Embryos that were sectioned for histology were fixed and embedded in JB-4 and plastic sections were preformed as described previously (Pack et al., 1996).

Whole-mount in situ hybridization

Embryos were collected and processed for whole-mount in situ hybridization as previously described (Thisse et al., 1993). Digoxigenin-labelled and fluorescein-labelled riboprobes were synthesized from templates linearized with *Bam*HI using T7 RNA polymerase for *trap100*. Other digoxigenin-labelled riboprobes used in this study were synthesized from templates linearized and transcribed as follows: *crestin* (Rubinstein et al., 2000), *Sac*I and T7; *phox2b* (Shepherd et al., 2004), *Not*I and T7; *dlx2a* (Akimenko et al., 1994) and *foxn1* (Schorpp et al., 2002), *Bam*HI and T7; *rag1* (Willett et al., 1997), *Hind*II and T7; *epha4* (Xu et al., 1995), *Eco*RI

and T3; *hoxb4* (Prince et al., 1998), *Kpn*I and T3; *ifbp* (Andre et al., 2000), *trypsin* (Mayer and Fishman, 2003), *pax9* (Nornes et al., 1996) and *gata6* (Pack et al., 1996), *Sal*I and T7; *foxa2* (Strahle et al., 1993), *Sac*I and T3; *ptc1* (Concordet et al., 1996), *Bam*HI and T3; *shh* (Ekker et al., 1995), *Hind*II and T7; *ret* (Bisgrove et al., 1997), *Not*I and T7; and *gfra1a* (Shepherd et al., 2001) and *nos1* (previously *nmos*) (Poon et al., 2003), *Not*I and Sp6. Digoxigenin-labelled probes were visualized with NBT/BCIP coloration reactions, while fluorescein-labelled riboprobe was visualized with Fast Red (Roche). Cross-sections of whole-mount in situ hybridized embryos were cut using a Reichardt Jung cryostat. Embryos were equilibrated in 20% sucrose in PBS solution and frozen in OCT. Sections (30 µm) were collected on Fisher super frost slides rehydrated in PBS and mounted in gel mount (Fisher).

Mapping and molecular analysis of *lsn*

The *lsn*^{w24} (AB background) mutation was mapped by out-crossing into the polymorphic wild-type strain WIK, followed by in-breeding of heterozygous progeny. We scanned the genome for linked SSLP markers by bulked segregant analysis using standard methods (Shimoda et al., 1999; Stickney et al., 2002; Talbot and Schier, 1999). This analysis placed the *lsn* mutation on linkage group 12 between z9891 and z4373, an interval of ~10 cM. Fine mapping using other SSLP markers and SNPs in 3'UTRs and intronic regions of ESTs that map to this region were used to further narrow the genetic interval. Using this approach, we identified one EST Fa05b04 for which we had 0 recombinants out of 1122 meiosis screened. This EST encodes a zebrafish *trap100*. We analyzed this candidate gene by complete sequencing of its cDNA isolated by RT-PCR from wild type and mutant embryos. The *trap100* cDNA isolated from mutants was found to have a base substitution at codon 189 of the 2970 codon open reading frame. This result was substantiated by sequencing PCR products from genomic DNA derived from 12 mutants, 12 phenotypically wild-type siblings as well as 12 unrelated wild types. The GenBank Accession Number for zebrafish *trap100* is DQ300265.

Embryonic microinjections

trap100 mRNA was synthesized using the mMessage mMachine kit (Ambion) and injected at a concentration of 50 ng/µl. The mRNAs were coinjected with *GFP* mRNA, also at a concentration of 50 ng/µl, to assess expression. Approximately 1 nl of diluted mRNA was injected into one- to two-cell embryos using a gas-driven microinjection apparatus (Model# MMPI-2; Applied Scientific Instrumentation) through a micropipette.

Morpholino antisense oligonucleotides (Gene Tools) were designed corresponding to the start site and the splice junction at the end of exon 3 of the genomic *trap100* sequence. The sequences were as follows: +1/+25, CCTGTTTCAGATTCACCACCTTCAT; +199/int 3, GTGTGTTTACCTGTGAAGTATGGC.

The oligos were resuspended in sterile filtered water and diluted to working concentrations at 1-5 µg/µl. Approximately 1 nl of diluted morpholino was injected into one- to two-cell embryos using a gas-driven microinjection apparatus. Efficacy of the morpholino directed against the splice junction of exon 3 was evaluated using RT-PCR with a forward primer corresponding to the 131 bp of *trap100* (AGCTCTTCTGGAGCAGGCTA) in conjunction with a reverse primer designed to 471 bp of *trap100* (GGCCCTCAGACTGCTTTCTA). *casanova* morpholino was designed to the previously described morpholino translation blocking sequence (Dickmeis et al., 2001).

Transplantation experiments

Donor and host embryos were generated from an in cross of *lsn* heterozygotes. Donor embryos at the one- to two-cell stage were injected with 1.5 pg of *Tar** mRNA combined with a mixture of 5% Biotin-dextran (10 K lysine fixable; Molecular Probes) and 5% fluorescein-dextran (10 K Lysine fixable; Molecular Probes) to convert most of the donor cells to an endodermal cell fate (Peyrieras et al., 1998). *Tar** mRNA were synthesized using the mMessage mMachine kit (Ambion) as described above. At the sphere stage, 20-40 donor cells were transplanted into unlabelled sibling host embryos. Embryos were then cultured in embryo medium with 10 U/ml penicillin and 10 U/ml streptomycin. Host embryo jaw cartilage development was determined on day 5 by Alcian Blue staining as described

above. Donor cells from the transplant were detected in hosts using an avidin-biotinylated complex (ABC kit, Vectastain) and a DAB substrate. Genotypes of the host and donor embryos were determined by sequencing.

RESULTS

lsn mutant isolation

In zebrafish, differentiated enteric neurons can be first detected at the anterior end of the intestine immunocytochemically at 72 hpf (Bisgrove et al., 1997; Kelsh and Eisen, 2000; Shepherd et al., 2001; Shepherd et al., 2004). By 96 hpf, enteric neurons can be identified along the complete length of the intestine. We screened ENU-mutagenized zebrafish for recessive mutations that interfere with the neurogenesis in the ENS. Clutches of embryos were obtained from pair-wise crosses of in-crossed F2 families. The clutches of embryos were immunocytochemically stained with an anti-Hu antibody (Marusich et al., 1994) to reveal differentiated neurons and then screened under a fluorescent microscope. We identified a mutant allele (*lsn*^{w24}) in which there was a significant reduction in the number of enteric neurons at 96 hpf (Fig. 1). *lsn* embryos have a 66% reduction in the number of enteric neurons over a 10-somite length segment stretching anteriorly from the cloaca (Fig. 3D). This reduction in enteric neurons in *lsn* mutants is more pronounced in the more distal part of the intestine when compared with the anterior part. Further analysis of subtypes of ENS neurons in *lsn* mutants, specifically serotonergic neurons by immunocytochemistry and nNOS-positive neurons by in situ hybridization, shows that there is a similar reduction in the number of these specific subtypes when compared with wild type at 96 hpf (see Fig. S1 in the supplementary material). These data suggest that different enteric neuron subtypes are equally affected in *lsn* mutants. Neuronal differentiation in other areas of the PNS appears normal in *lsn* mutants. The dorsal root ganglia, sympathetic neurons and cranial ganglia are present and are comparatively normal at 96 hpf, based on anti-Hu immunocytochemistry (Fig. 3; see Fig. S2 in the supplementary material). Further analysis of cranial ganglia development by in situ hybridization using a *phox2b* probe (Elworthy et al., 2005) also shows that the ganglia are normally specified at 48 hpf (see Fig. S2 in the supplementary material). The mutation is recessive lethal and 100% penetrant in all backgrounds tested (AB and WIK). Mutant embryos die by 7 dpf. We called the mutant *lessen* (*lsn*) as the mutants had less enteric neurons than wild type.

lsn mutants also have other defects in structures that are derived completely or receive cellular contributions from the neural crest. The most severely affected structures appear to be predominantly those that are derived from or receive contributions from the vagal/post-otic neural crest cells (Lam et al., 2002; Schilling and

Kimmel, 1994). At 5 dpf *lsn* mutants fail to develop the most posterior ceratobranchial cartilages (cb 4,5), while the more anterior ceratobranchial cartilages and the other anterior cartilages of the jaw are less severely affected (Fig. 2A-D). In addition, there is cardiac oedema apparent from 96 hpf and the thymus primordium appears not to form normally, based on reduced Rag1 in situ expression (Fig. 2E,F) (Willett et al., 1997). Whether the cardiac or thymus defects are due to neural crest defects has not been determined.

Other neural crest derived tissues appear unaffected in *lsn* mutants. We detected no difference in the normal pattern of melanophores or iridophores by light microscopy at 96 hpf (Fig. 1). In situ hybridization studies using in situ probes for *sox10* (Dutton et al., 2001) and *nacre* (Lister et al., 1999) at 24 hpf revealed no detectable difference in the pattern of expression of these two markers, suggesting that neural crest derived pigment cell development is unaffected in *lsn* (data not shown). We also examined the pattern of *sox10* at 48 hpf as a marker of glial cells along the posterior lateral line (Kelsh and Eisen, 2000) and detected no difference in the pattern of staining in *lsn* when compared with wild type (data not shown). Together this suggest that the *lsn* mutation does not affect all neural crest-derived tissues but instead affects specific axial subpopulations of neural crest cells.

The *lsn*^{w24} mutation disrupts a zebrafish *trap100*

We identified the affected gene disrupted in *lsn* by mapping and molecular analysis of the *lsn*^{w24} mutation. Genetic mapping localized *lsn* to linkage group 12 (LG.12) between markers z9891 and z4373 (Fig. 3A). By scoring 1122 meioses, we established a fine map of the region using both microsatellite markers and SNPs in the 3'UTR or intronic regions of known genes or ESTs that had been mapped to this the crucial interval. Using this approach, we identified a zebrafish EST (fa05b04) that had no recombinants out of the 1122 meioses. Sequence analysis suggested that fa05b04 encoded a zebrafish homologue of Trap100, a component of the Trap/mediator transcriptional regulation complex (Malik and Roeder, 2000; Myers and Kornberg, 2000; Rachez and Freedman, 2001). We cloned and sequenced this gene and verified by sequence comparison of the complete ORF that we had identified a zebrafish *trap100* orthologue of mouse and human *Trap100/TRAP100* (*Thrap4/THRAP4*; Mouse Genome Informatics and Human Gene Nomenclature Database) (Fig. 3B) (Yuan et al., 1998; Zhang and Fondell, 1999).

To determine if there was a mutation in this *trap100* orthologue in *lsn*, we used RT-PCR to amplify the complete ORF of the zebrafish *trap100* gene from genotypically homozygous wild-type and homozygous mutant 48 hpf embryos. Sequencing of these RT-PCR products revealed that the *lsn* mutant *trap100* has a T to A base

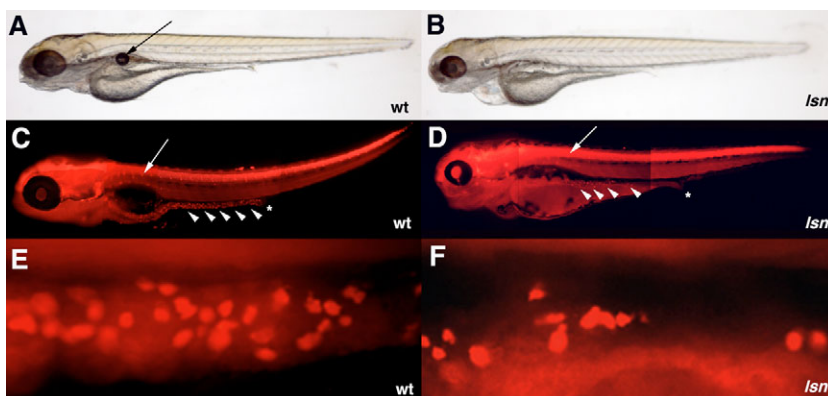


Fig. 1. *lsn*-mutant phenotype. (A,B) Lateral views of live larvae at 96 hpf, showing the abnormal development of the jaw, eye and heart in *lsn* (B) when compared with wild type (A), and lack of swim bladder in *lsn*. Arrow in A indicates the swim bladder. (C,D) Lateral views of 96 hpf embryos stained with anti-Hu antibody shows normal DRG development in *lsn* but a reduced number of enteric neurons that are absent from the distal end of the gut tube. Stars indicate the end of the gut tube; arrows indicate DRGs; arrowheads indicate enteric neurons. (E,F) Lateral views of the gut tube of 96 hpf embryos stained with anti-Hu antibody showing reduced number of neurons in *lsn*.

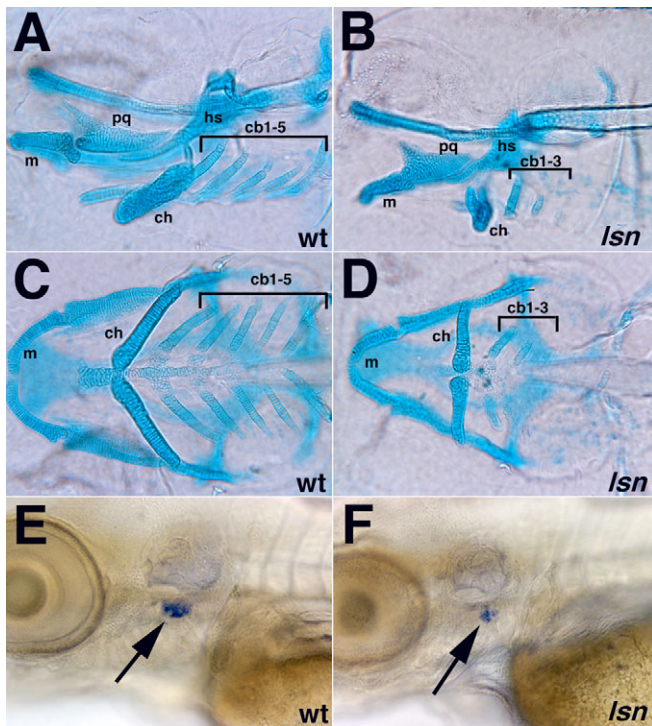


Fig. 2. *lsn* mutation affects both craniofacial and thymus development. (A-D) Alcian Blue staining showing pharyngeal cartilages in 120 hpf wild-type (A,C) and *lsn* mutant (B,D) larvae shown in lateral (A,B) and ventral (C,D) views. In *lsn*, the development of the pharyngeal cartilages is abnormal. Notably the ceratobranchials 4 and 5 are absent in *lsn*. cb 1-5, ceratobranchial cartilages 1-5; ch, ceratohyal cartilage; hs, hyosymplectic cartilage; m, Meckel's cartilage; pq, palatoquadrate cartilage. (E,F) *rag-1* expression at 96 hpf in wild-type (E) and *lsn* mutant (F) larvae shows that *lsn* embryos have a significantly reduced thymic primordia (arrows).

substitution that results in a premature stop codon at amino acid 63 in the N-terminal part of protein (Fig. 3C). This base is located in the third exon of the *trap100* gene. Sequencing of this exon from genomic DNA isolated from morphologically identified 96 hpf *lsn* mutant embryos showed that all homozygous mutant embryos have this base substitution, while all homozygous wild-type siblings lack this base change. As the predicted Trap100 protein made in *lsn* mutants will be severely truncated (63 amino acids long as opposed to 989) and all the predicted functional domains will be missing in this truncated protein, we believe that *lsn* is a null allele of *trap100*.

As a further demonstration that *trap100* is responsible for the *lsn* phenotype, we performed rescue experiments using mRNA and cDNA that encoded wild-type *trap100*. To score the effectiveness of the rescue, we counted the number of enteric neurons in a 10-somite segment of the intestine stretching anteriorly from the anus. Microinjection of either *trap100* mRNA or cDNA into embryos at the one- to two-cell stage partially rescued the number of enteric neurons in homozygous mutant embryos when compared with control injected embryos (Fig. 3D; data not shown). No overexpression phenotype was observed when mRNA or cDNA was injected into heterozygous and homozygous wild-type siblings (Fig. 3D and data not shown).

To provide additional evidence that reduction in *trap100* function causes the *lsn* phenotype, we injected one-to-two-cell stage embryos with a morpholino antisense oligonucleotide directed against the

putative translation start site of the gene or with a splice-blocking morpholino directed against the splice donor site at the end of exon 3. Injection of either morpholino resulted in jaw morphology, cardiac oedema and the enteric phenotypes similar to those displayed by *lsn* mutants (Fig. 4). The morphant phenotypes were the same for both morpholinos. In the case of the splice-blocking morpholino, the morphant phenotype correlated with a dramatic change in *trap100* transcripts in which adjoining introns are not spliced correctly as detected by RT-PCR using primers that amplify over these splice sites (data not shown). Notably, morpholino injections did not increase the severity of phenotype when injected into homozygous *lsn*^{w24} mutants, supporting the notion that *lsn*^{w24} is a complete loss-of-function mutation.

***trap100* expression**

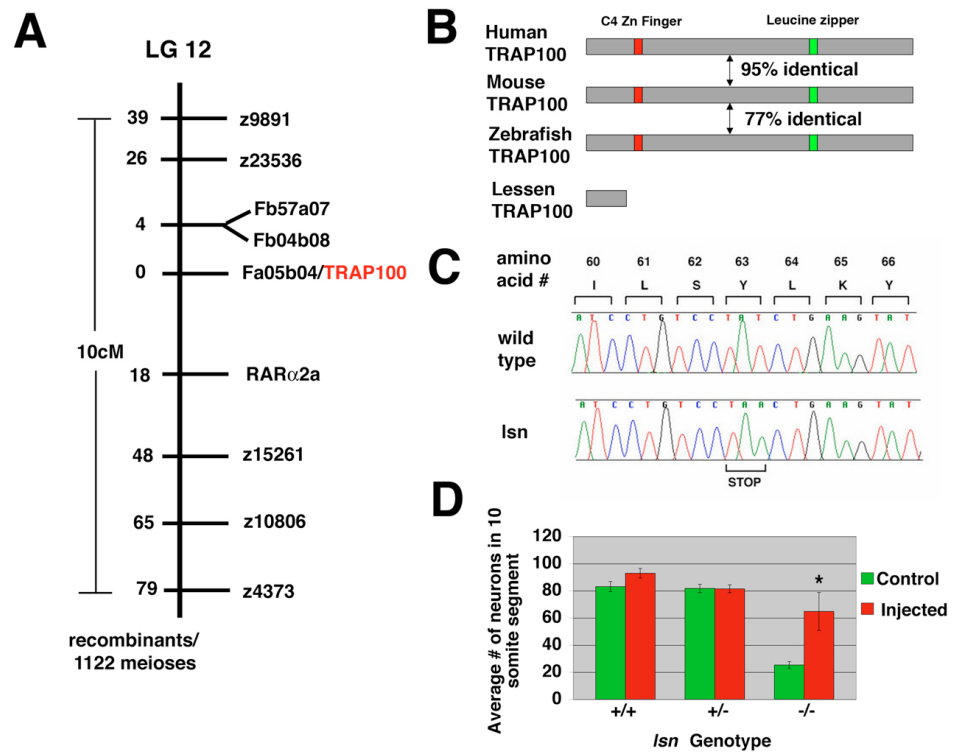
Zebrafish *trap100* is maternally expressed as determined by RT-PCR and in situ hybridization. Through the 10-somite stage, expression is ubiquitous (Fig. 5A-C). Subsequently *trap100* expression starts to become more restricted with expression becoming reduced in the trunk and tail tissue while remaining high in more anterior parts of the embryo. By 24 hpf *trap100* is no longer detected in the trunk and tail (Fig. 5D,E). Widespread expression is maintained in anterior parts of the embryo in both neural and non-neural tissue extending the length of the hindbrain including through out the pharyngeal arches. Expression is also present in the anterior parts of the gut tube. The pattern of expression at 48 hpf is essentially the same as that seen at 24 hpf but expression now extends along nearly the complete length of the gut (Fig. 5F). Cross-sections taken at the level of somite 4 show that the expression in the gut is throughout the mesendoderm (Fig. 5G). Although expression remains widespread throughout the neural and non-neural tissue in anterior parts of the embryo, three areas of higher expression of *trap100* can be seen in the CNS: in the dorsal forebrain, in the ventral midbrain and in a stripe of expressing cells in the dorsal posterior part of the midbrain (Fig. 5F). At 60 hpf, cross-sections through the anterior part of the gut show that *trap100* expression is restricted to intestinal epithelial cells (Fig. 5H,I). Double-label in situ hybridization studies using a *trap100* probe in conjunction with a *phox2b* probe show that *trap100* is not expressed in the ENS precursors (Fig. 5H,I). By 72 hpf expression of *trap100* becomes much more restricted (Fig. 5J,K). Expression in the CNS is restricted to discrete groups of cells in the diencephalon, in the ventral midbrain and in a stripe of cells in the dorsal posterior part of the midbrain. Weak expression can also be detected in the retina predominantly restricted to the margin. Outside of the CNS expression becomes restricted to the pharyngeal endoderm. This expression extends into the most anterior part of the gut endoderm but does not extend to more posterior parts of the gut. Pharyngeal endoderm expression is maintained through 96 hpf, the latest age we examined in the present study (data not shown).

***trap100* is not required for endoderm-intestinal transition**

To determine whether the enteric defect was also associated with other defects in intestinal development we examined cross-sections of mutant embryos (Fig. 6A,B). At 96 hpf, the gut tubes of the mutant embryos appear smaller and less well organized when compared with wild-type and heterozygous siblings. Similarly, the liver and pancreas are present in the mutant embryos but they are reduced in size when compared with their wild-type siblings. We examined the expression pattern of several early markers of intestinal development by in situ hybridization, including *foxa2* (Odenthal and Nusslein-Volhard,

Fig. 3. Positional cloning of *lsn*.

(A) *lsn*^{w24} maps on to linkage group 12 between markers z9891 and z4373. No recombinants were found between *lsn*^{w24} and a SSCP marker in the 3' UTR of an EST (Fa05b04) that encodes for a zebrafish *trap100*. We isolated a full-length cDNA corresponding to *trap100* from homozygous-*lsn* mutant and wild-type embryos and 12 independent clones were completely sequenced in both directions. A T to A (encoding Y to stop) mutation was identified in *trap100* cDNAs derived from homozygous-*lsn* mutants. (B) A schematic illustrating the overall structure and percentage similarity between human, mouse and zebrafish Trap100, and the predicted truncated Trap100 in *lsn* mutants. (C) Sequence tracing of one of the 12 independent clones derived from genomic PCR of genomic DNA from mutant and wild-type embryos showing TAA (stop) mutation. (D) A bar graph showing rescue of the *lsn* homozygous mutant enteric phenotype by injection of wild-type *trap100* mRNA. Embryos derived from an incross of heterozygote *lsn* fish were injected with 50 pg of *trap100* mRNA, fixed and stained with anti-Hu antibody at 96 hpf and genotyped. Control represents genotyped uninjected embryos from the same cross. Total number of enteric neurons in a 10-somite segment of the intestine were counted. Numbers represent the mean number of enteric neurons in this 10-somite segment ± s.e.m. for 15 embryos of each genotype for each condition. *Significantly different from control (Student's *t*-test *P*<0.001).



1998; Strahle et al., 1993), *gata6* (Pack et al., 1996), *shh* (Ekker et al., 1995; Roy et al., 2001) and *ptc1* (Concordet et al., 1996; Lewis et al., 1999) in genotyped wild-type and *lsn* homozygous mutant embryos. No difference was detected in the expression pattern of these genes (data not shown). To determine if the reduction in size of the gut tube and the pancreas seen at 96 hpf was associated with a failure of these organs to functionally differentiate, we carried out an in situ analysis using probes to *trypsin* and *intestinal fatty acid binding protein (ifbp)* (Fig. 6C-F) (Andre et al., 2000; Mayer and Fishman, 2003). Both genes were expressed in *lsn/trap100* mutants in comparatively normal expression patterns, suggesting that the gut tube and the pancreas have undergone cytodifferentiation into more mature organs, unlike the recently identified *npo* mutant (Mayer and Fishman, 2003). Although differentiation has occurred normally, the normal looping of the gut has failed to occur, leading to an apparent straight gut tube (Fig. 6F). Together, these results suggest that, although gut and intestinal organ development is less advanced in the *lsn* mutants, there has been no arrest in intestinal development and that *lsn/trap100* is not essential for the differentiation of intestinal endoderm derivatives.

***trap100* is not required for neural crest specification or initial migration and patterning**

To determine the point at which neural crest development is disrupted in *lsn*, we analyzed the expression of molecular markers of the premigratory and migrating neural crest. By gross morphology, *lsn* mutants appear normal until about 84 hpf. There is no difference in the specification or the initial migration of the cranial neural crest in *lsn* mutants when compared with wild-type siblings as determined by in situ using the pan-crest specific marker

crestin (Luo et al., 2001; Rubinstein et al., 2000) or by using other neural crest markers Sox10 and Foxd3 (see Fig. S3 in the supplementary material; data not shown). Furthermore, no

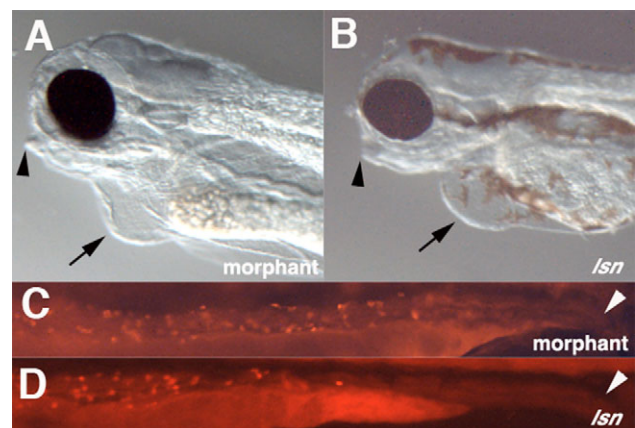


Fig. 4. Effect of *trap100* antisense morpholino oligonucleotide injection on jaw, heart and enteric neuron development.

(A,B) Lateral views of the heads of 96 hpf *trap100* morphant (A) and *lsn* mutant (B) embryos. Arrowheads indicate the recessed jaw; arrows indicate cardiac oedema. (C,D) Lateral views of the intestines of 96 hpf embryos stained with anti-Hu antibody. Arrowheads indicate the end of the intestine. The lack of melanophores in morphant the embryo (A) is not due the effect of the *trap100* morpholino. Embryos injected with the *trap100* morpholino were obtained from an incross of *nacre* homozygous fish (Lister et al., 1999) and lack melanophores because of a mutation in *mitfa*.

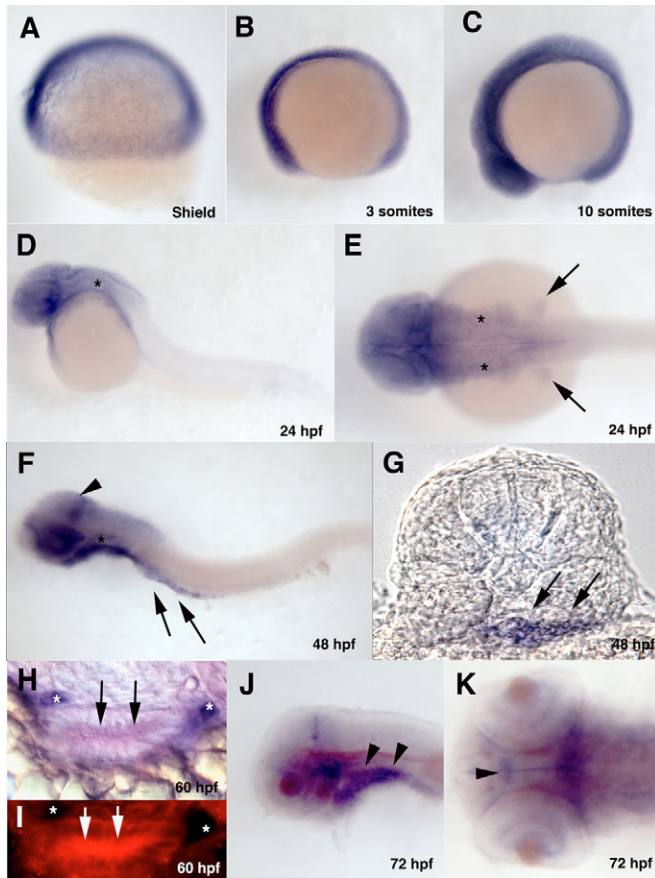


Fig. 5. Developmental expression pattern of *trap100*. (A-F) Whole-mount in situ hybridized embryos hybridized with a *trap100* antisense probe at the indicated developmental stages. (A-D,F) Lateral views; (E) Dorsal view of 24 hpf embryo. Asterisks in D-F indicates the otic vesicle. Arrows in E indicate fin buds. Arrowhead in F indicates increased expression of *trap100* in the posterior mesencephalon. Arrows in F indicate intestinal mesendodermal expression of *trap100*. (G) A transverse section taken through 48 hpf embryo at the level of somite 4 showing expression through the intestinal mesendoderm. Arrows indicate intestinal mesendodermal expression of *trap100*. (H) A transverse section taken through the gut tube at 60 hpf after double in situ hybridization with a *trap100* fluorescein antisense probe (red) and a *phox2b* digoxigenin antisense probe (purple) showing intestinal epithelia expression of *trap100*. (I) Same section as in H showing *trap100* expression using fluorescence in the intestinal epithelia cells. Arrows and asterisks in H,I indicate intestinal mesendodermal expression of *trap100* and *phox2b*-positive ENS precursors, respectively. (J,K) Whole-mount in situ hybridized embryos hybridized with a *trap100* antisense probe at 72 hpf. (J) Lateral view; (K) dorsal view. Arrowheads in J indicate pharyngeal arch mesendodermal expression. Arrowhead in K indicates ventral diencephalon cells expressing neurons expressing *trap100*. In all whole mounts (A-F,J,K), anterior is towards the left; (F,K,J) yolk has been removed.

difference is detected in the patterning of the hindbrain from which the cranial crest neural crest arises as detected by in situ hybridization using *epha4* and *hoxb4* (Prince et al., 1998; Schilling and Kimmel, 1994; Xu et al., 1995) (see Fig. S3 in the supplementary material).

We subsequently analyzed the migration and initial patterning of the jaw cartilages and the patterning of the thymus in genotyped embryos to determine if these structures had early

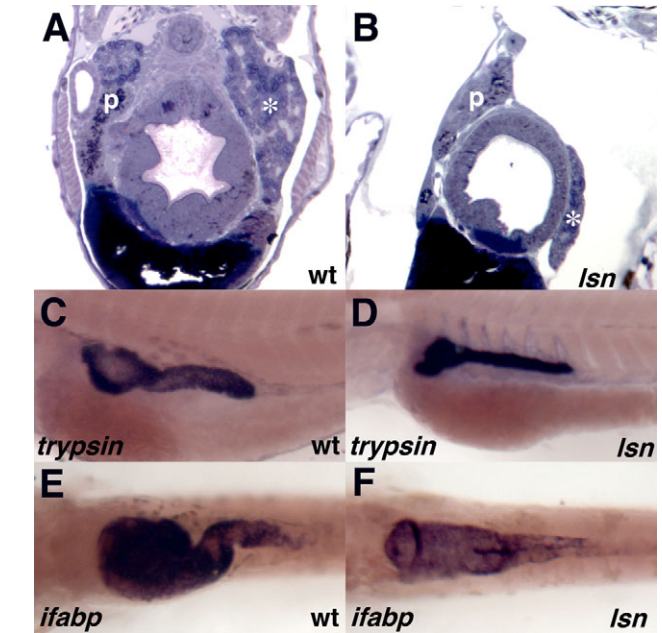


Fig. 6. *trap100* is required for normal intestinal development but is not required for endoderm-intestine transition. (A,B) Cross-sections of 120 hpf wild-type (A) and *lsn* mutant (B) embryos stained with Toluidine Blue. (C,D) *trypsin* expression at 96 hpf in whole-mount in situ hybridized wild-type (C) and *lsn* mutant (D) embryos. (E,F) *ifabp* expression at 96 hpf in whole-mount in situ hybridized wild-type (E) and *lsn* mutant (F) embryos. p, pancreas; *, liver.

defects in crest precursor migration or specification. No difference is observed in the migration of neural crest precursors to the jaw using a *dlx2a* (Akimenko et al., 1994) in situ probe or in their initial differentiation as determined by the expression of *pax9* (Nornes et al., 1996) (see Fig. S4 in the supplementary material). Furthermore, no difference is observed in the initial patterning and specification of the thymus at 48 hpf, as determined using an in situ probe for the early thymus marker *Foxn1* (Schorpp et al., 2002) (see Fig. S4 in the supplementary material).

We next examined the initial migration of the enteric precursors to the gut tube from the vagal region by in situ hybridization using the pan-crest specific marker *crestin* (Luo et al., 2001; Rubinstein et al., 2000) (Fig. 7A,B) or using more specific enteric precursor markers *gfal1a* and *ret* (data not shown) (Bisgrove et al., 1997; Shepherd et al., 2004). No difference in the expression of these markers is detected prior to 48 hpf. However, at 48 hpf a difference in ENS development can be detected. In wild-type embryos, ENS precursors can be seen along the entire length of the intestine at 48 hpf (Fig. 7C) (Shepherd et al., 2004). By contrast, in *lsn* homozygous mutants enteric precursors have only migrated to the anterior part of the intestine by 48 hpf (Fig. 7D). The lack of enteric precursor cells in the more posterior parts of the intestine is maintained at 60 and 72 hpf, as determined both by in situ using probes for *phox2b* (Elworthy et al., 2005; Shepherd et al., 2004), *gfal1a* (Shepherd et al., 2001), *ret* (Bisgrove et al., 1997) and *nos1* (Poon et al., 2003), and by immunocytochemistry using an anti-*phox2b* antibody (Pattyn et al., 1997) (Fig. 7E-H; Fig. 8A,C). These results are consistent with the Hu immunocytochemistry that was used to identify the *lsn* mutants (Fig. 1D,F).

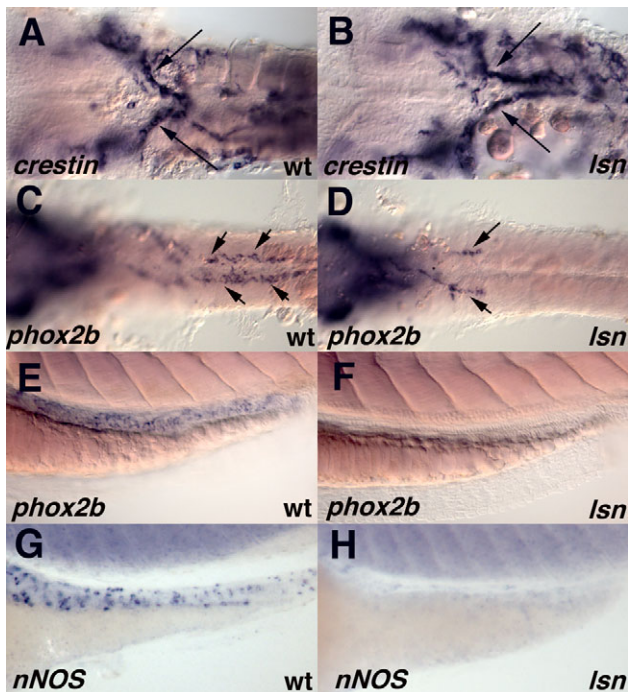


Fig. 7. *lsn* mutation causes a failure of enteric precursors to populate the entire length of the intestine but does not perturb the initial migration of vagal neural crest to the anterior gut. (A,C,E,G) Wild-type and (B,D,F,H) *lsn* mutants embryos. Anterior is towards the left. (A,B) Ventral view of the vagal region of 36 hpf embryos hybridized with riboprobes for *crestin*. (C,D) Ventral view of the vagal region to somite 10 of 48 hpf embryos hybridized with riboprobes for *phox2b*, showing a failure of *phox2b*-expressing cells to populate the entire length of the intestine. Arrows indicate the migrating enteric precursors. The yolk has been removed from the embryos (A-D). (E-H) Lateral views of the intestine, 72 hpf wild-type (E,G) and *lsn* mutant (F,H) embryos hybridized with riboprobes for *phox2b* (E,F) and *nos1* (previously *nnos*) (G,H).

Proliferation of migrating ENS precursors in the intestine is reduced in *lsn* mutants

Our results imply that the initial formation and specification of ENS precursors from the premigratory vagal neural crest as well as the initial migration of ENS precursors to the anterior end of the intestine is normal in *lsn* embryos. Similarly, these data suggest that the initial specification and patterning of the other neural crest-derived structures is not overtly perturbed in the *lsn* mutant.

To determine why the ENS precursors subsequently fail to populate the entire length of the intestine, we examined whether this phenotype resulted from an absence or reduction in *gdnf* expression along the intestinal mesendoderm. Previously, we have shown GDNF is crucially required for ENS precursor migration along the intestine (Shepherd et al., 2001). *gdnf* expression is unchanged in *lsn* mutants when compared with wild type (see Fig. S5 in the supplementary material). This result combined with the observation that *lsn* ENS precursors have a normal expression of GDNF receptor components suggests the *lsn* ENS phenotype does not result from a perturbation of this signalling pathway.

To determine whether the *lsn* ENS phenotype resulted from an increase in cell death of ENS precursors, we examined whether there was an increase in the number of cells undergoing apoptosis

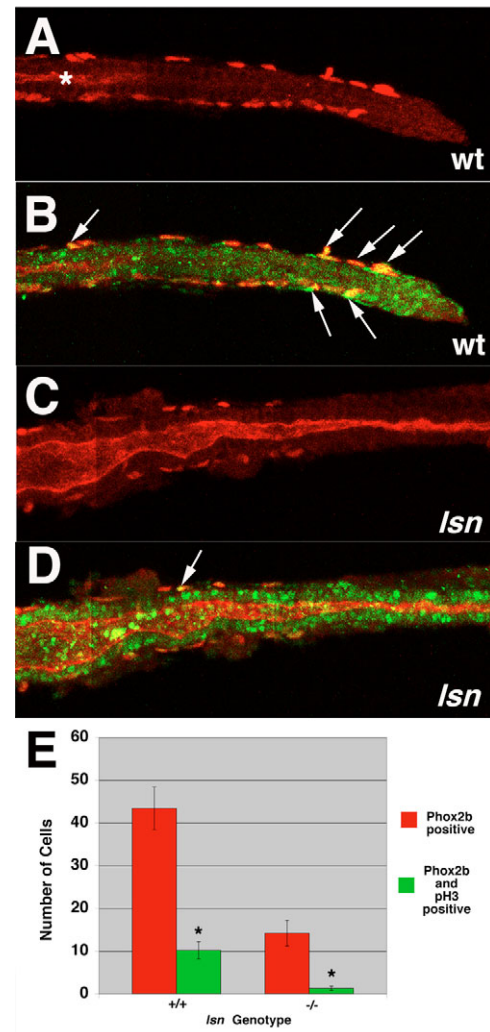


Fig. 8. *lsn* mutants have reduced ENS precursor proliferation. (A-D) Confocal images of dissected intestines from 48 hpf wild-type (A,B) and *lsn* (C,D) embryos immunocytochemically stained with anti-Phox2b antibody (red) and anti-phosphohistone H3 antibody (green). (A,C) Anti-Phox2b immunoreactivity in wild type (A) and *lsn* (C), showing the most posterior point along the gut tube that Phox2b-positive cells can be identified. (B,D) Merged images of the intestines in A and C showing anti-Phox2b and anti-phosphohistone H3 immunoreactivity (arrows). Asterisk in A indicates the end of the gut lumen, which is not opened up to the distal end of the gut tube at this developmental age. Arrows in B,D indicate double-labelled cells. (E) Bar graph showing the mean number of Phox2b immunoreactive cells (red) and double-labelled Phox2b/phosphohistone H3 positive cells (green) present along the entire length of the intestine of 48 hpf wild-type and homozygous mutant *lsn* embryos. Embryos derived from an incross of heterozygote *lsn* fish were fixed and stained with anti-Phox2b and anti-phosphohistone H3 antibodies at 96 hpf and genotyped. Numbers represent the mean number of immunopositive cells \pm s.e.m. for 10 embryos of each genotype. The difference between them was statistically significant (Student's *t*-test, **P* < 0.001).

in the intestine of 48 and 72 hpf *lsn* embryos when compared with wild-type siblings using TUNEL assay (Gavrieli et al., 1992). At both ages, we observed very few cells undergoing apoptosis in the intestines of either wild-type or *lsn* mutant embryos, consistent with the recent study by Ng et al. (Ng et al., 2005) (see Fig. S5 in

the supplementary material). We determined that there is no difference between the number of cells undergoing apoptosis in the intestine of mutant embryos and wild-type siblings at either age.

Given the absence of an increase in the number of cells undergoing apoptosis in the intestine of *lsn* mutants, we examined whether the phenotype resulted from a decrease or lack of in proliferation of ENS precursors once they reached the intestine. As previously noted, *lsn* mutants have a significant reduction in the number of ENS precursors in the intestine at 48 hpf as detected by Phox2b immunocytochemistry (Fig. 8) and by other ENS precursors specific markers using in situ hybridization (Fig. 7 and data not shown). By undertaking double label immunocytochemistry with the Phox2b antibody and an antibody for phosphohistone H3, a marker of proliferating cells (Ajiro et al., 1996), we determined that there is a 88% reduction in the number of proliferating ENS precursors at 48 hpf (Fig. 8E). This result suggests that the decrease in the number of ENS precursors seen at 96 hpf is caused at least in part by the reduction in ENS precursor proliferation.

lsn/trap100 is required non-cell autonomously for pharyngeal arch neural crest cells

As *lsn/trap100* mutants exhibit defects in the neural crest derived head skeleton and *trap100* is widely expressed through out the pharyngeal arch mesendoderm we tested whether *lsn/trap100* is required only in the mesendoderm. We attempted to rescue *lsn/trap100* mutant cartilages by placing wild-type cells into the pharyngeal mesendoderm. Transplantation of unmanipulated wild-type cells usually results in small mesendodermal clones. To achieve larger clones in endodermal pouches, we injected wild-type donors prior to transplantation with *Tar**, an activated version of the type I TGF β -related receptor Taram A (Tar) to convert blastomeres to an endodermal fate (David and Rosa, 2001; David et al., 2002; Peyrieras et al., 1998) (Fig. 9A). As expected, donor cells in the mosaic embryos contribute largely to the pharynx, endodermal pouches of the pharyngeal arches and only very rarely to the entire length of the digestive tract. In seven out of nine *lsn* larvae (78%) in which transplanted wild-type cells contributed to the mesendoderm of the pharyngeal arches partial rescue of the most posterior ceratobranchial cartilages (3, 4, 5) was observed (Fig. 9C). Rescue corresponded only to regions where transplanted cells contributed to the pharyngeal pouch endoderm. These results suggest that the cartilage defects in *lsn/trap100* result from defect signalling from the endoderm.

Endoderm is required for the normal development of the ENS

To determine whether endoderm is necessary for the development of the ENS we injected zebrafish embryos with a specific MO directed against *casanova* (*cas*) mRNA (Dickmeis et al., 2001). *Cas* is a Sox-related factor that is required for endoderm formation (Alexander et al., 1999; Dickmeis et al., 2001; Kikuchi et al., 2001). All *Cas*-MO-injected embryos exhibited cardiabifida and completely lacked intestinal endoderm as determined by *foxa3* expression (Fig. 9F,H). When compared with uninjected controls, *cas* morphants completely lacked *phox2b* expression in the ENS precursors, while expression in the hindbrain remained though the pattern of expression was altered. To confirm that this was not just a developmental delay, we stained 96 hpf *Cas*-MO embryos with anti-Hu antibodies. No Hu immunoreactivity was seen in the ventral region of the embryo where the ENS neurons normally are located (data not shown). These experiments demonstrate that endoderm is required for the development of the ENS.

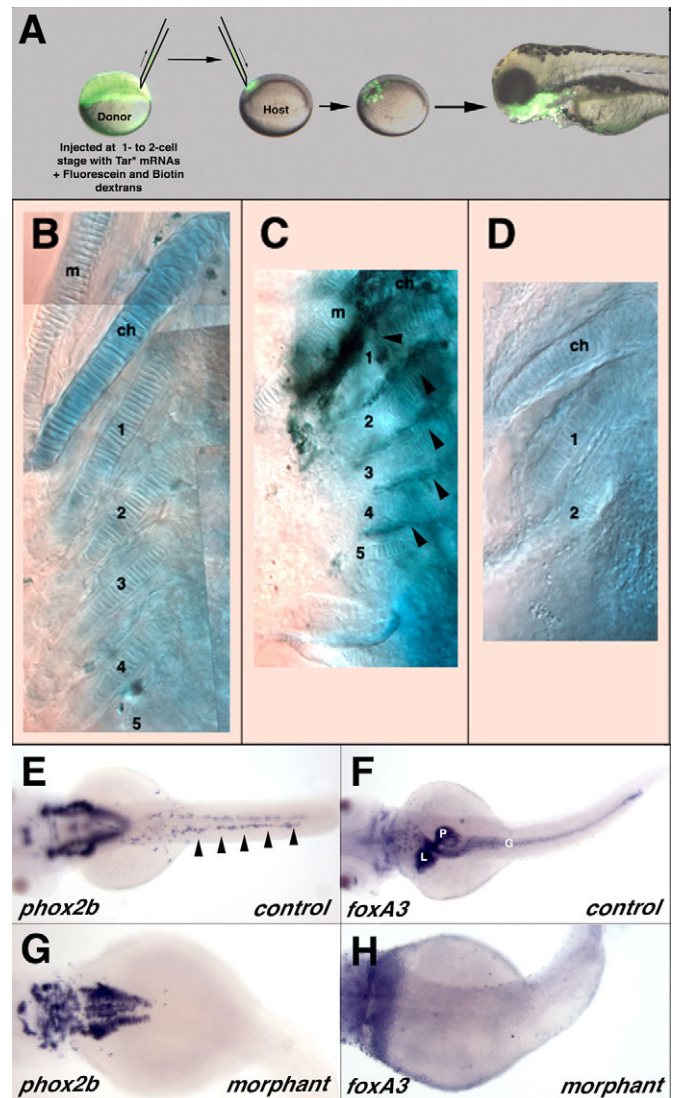


Fig. 9. Transplants suggest that *lsn*^{w24} functions cell autonomously in the endoderm and endoderm is required for ENS development. (A-D) Transplantation of wild-type endodermal cells partially rescues posterior arch cartilage formation in *lsn* mutants. (A) At blastula stage, fluorescein-dextran labelled wild-type cells expressing *Tar** were transplanted into host and allowed to develop. The lateral view of the head region at 72 hpf shows grafted cells (green) have differentiated into pharyngeal endoderm derivatives. (B-D) Ventral views of 5 dpf larvae stained with Alcian Blue to show cartilages. (B) Wild-type control. All lower jaw cartilages are clearly identifiable. (C) *lsn* mutant larvae transplanted with wild-type cells showing rescue of posterior ceratobranchial (3-5) in the vicinity of transplanted *Tar**-expressing wild type cells (black staining) in the pharyngeal arch endoderm (arrowheads). (D) *lsn* mutant that lacks posterior ceratobranchials. (E-H) *Casanova* morphant embryos have no intestinal endoderm and no migrating ENS precursors. Dorsal views of 48 hpf control embryos (E,F) and *cas* morphant embryos (G,H) hybridized with riboprobes for *phox2b* (E,G) or *foxa3* (F,H) showing a complete lack of *phox2b*-expressing cells in the region of the intestine of morphant embryos (G) that also completely lack intestinal endoderm (H). Arrowheads in E indicate migrating ENS precursors. m, Meckel's cartilage of the mandibular arch; ch, ceratohyal cartilage; 1-5 ceratobranchial cartilages; G, intestine; L, liver, P, pancreas.

DISCUSSION

In this study, we show that *lessen* (*lsn*) is a mutation in a zebrafish *trap100* gene that is orthologous to genes identified in mouse and human (Yuan et al., 1998; Zhang and Fondell, 1999). Trap100 is required for the normal development of specific neural crest-derived structures in zebrafish. The lesion in *lsn* is a point mutation in *trap100* that introduces a stop codon in the third exon of the gene and is predicted to severely truncate the mutant protein. We predict that the *lsn* mutation results in a *trap100*-null phenotype as the *lsn* Trap100 protein lacks all its predicted functional domains. Consistent with this, injection of two different morpholinos, a translation blocking morpholino or a splice-blocking morpholino, into *lsn* mutants does not result in a more severe phenotype, indicating that *lsn* is a complete loss-of-function mutant. We show that Trap100 is required for the normal proliferation of ENS precursors but not for the initial specification and migration of the ENS precursors to the anterior end of the intestine. In mice, disruption of *trap100* results in an early embryonic lethal phenotype at E9-10, primarily thought to be due to placental development defects that result in anaemia and poor nutritional supply, but also due to defects in overall cell growth through out the embryo (Ito et al., 2002). Because of this early embryonic lethality in the *Trap100*^{-/-} mouse, a crucial role for Trap100 in ENS development as well as the normal development of other vagal neural crest derived structures was previously unrecognized.

***trap100* has tissue specific functions during embryogenesis**

Previous genetic studies of murine TRAP/mediator complex components TRAP220 (Ito et al., 2000; Zhu et al., 2000), SRB7 (Tudor et al., 1999) and Trap100 (Ito et al., 2002) have shown that the complex is essential for embryogenesis but the genetic null mutant mice have different degrees of phenotypic severity, with *Srb7*^{-/-} mice having the most severe phenotype with embryos only reaching the blastocyst stage whereas *Trap220*^{-/-} mice are viable up to E11. This variation has led to the proposal that although the TRAP/mediator complex is essential for normal cell viability, cells that express TRAP/mediator complexes with different subunit compositions may have more specific roles regulating tissue specific transcription for those cell types with that subunit composition (Ito et al., 2002).

Our finding that the *lsn* mutant is viable until larval stages of zebrafish development (7 dpf) is surprising given the early Trap100-null mouse lethality (Ito et al., 2002). Furthermore, the zebrafish Trap100-null phenotype does not exhibit similar defects in the spatiotemporal organization and proliferation in the neural tube and cardiovascular system as reported in the Trap100-null mouse (Ito et al., 2002). By contrast, the *lsn* mutant phenotype clearly shows a tissue-specific role for Trap100 in both ENS/intestinal development as well as in jaw development. The jaw development phenotype is not unique for mutations that affect TRAP/mediator components. Haploinsufficiency in the TRAP/mediator subunit PAQ/ARC105 in DiGeorge syndrome indicates a potential specialized role in development of organs derived from the first and second branchial arches though the crucial role of *Tbx1* also deleted in this deficiency is thought to be the critical gene that causes the branchial arch phenotype in DiGeorge (Berti et al., 2001; Jerome and Papaioannou, 2001; Lindsay et al., 2001; Merscher et al., 2001). The *lsn* mutant phenotype potentially has revealed a role for Trap100 in the development of posterior branchial arch derived cartilages. The differences between the mouse and zebrafish Trap100-null phenotypes probably have arisen due to the crucial role of Trap100

in placental development in amniotes (Ito et al., 2002). Clarification as to whether this phenotypic difference is due to the placental defect could be revealed using mouse chimera studies. It is also possible that this difference occurs due to maternally deposited Trap100 protein rescuing any early defects in *lsn* mutants.

***trap100* function in endoderm is required for normal development of neural crest derived pharyngeal structures**

In this study, we show that the *lsn* posterior jaw cartilage mutant phenotype can be rescued by transplantation of wild-type endodermal cells. This result suggests that signals from the pharyngeal mesendoderm required for the normal development of the neural crest-derived cartilages are either reduced or missing. Pharyngeal cartilage development is a complex process requiring inductive signals from the surrounding endoderm and ectoderm (Couly et al., 2002; Crump et al., 2004a; Crump et al., 2004b; Hall, 1980). A large number of genes are expressed in pharyngeal arches during embryogenesis, underscoring the genetic complexity of their development. A number of these genes are expressed in an evolutionarily conserved manner in zebrafish (Yelick and Schilling, 2002) and several of these genes have been shown to affect pharyngeal pouch segmentation and jaw cartilage development including *fgf3* (Crump et al., 2004a; David et al., 2002), *fgf8* (Crump et al., 2004a) and *tbx1* (Piotrowski et al., 2003). The migration of the neural crest into the branchial arches is unaffected in *lsn* mutants, suggesting that pharyngeal pouch segmentation is normal and that expression of these genes is unaffected in *lsn*. Consistent with this supposition is our data showing that the development of the epibranchial placodes is normal in *lsn* (see Fig. S2 in the supplementary material). This is a process that has recently been shown to be endoderm dependent (Holzschuh et al., 2005; Nechiporuk et al., 2005). Further investigation will be required to determine if other signalling molecules, such as endothelin 1, that are known to play an essential role in pharyngeal cartilage specification and differentiation are affected in *lsn* (Kimmel et al., 2003; Miller et al., 2000; Piotrowski et al., 2003).

***trap100* is required for proliferation of vagal neural crest derived ENS precursors**

In this study, we show that the *lsn* ENS phenotype is due to a reduced level of proliferation of the ENS precursors. The findings that there is a reduced number of ENS precursors from the onset of migration along the gut and that fewer of these precursors are proliferating are consistent with the later reduction in the total number of enteric neurons seen at 96 hpf. Interestingly, we observe that in wild-type embryos, the majority of phosphohistone H3-positive ENS precursors are the most caudal migrating ones. This observation raises the possibility that the migration of ENS precursors along the gut is a proliferative migration, i.e. it is a combination of cells actively moving distally along the intestine combined with an increased number of new ENS precursors being generated specifically at the leading edge of the migration. This is not apparent in the mouse, where there appears to be no significant increase in proliferation in precursors at the leading edge of the wave of migration (Young et al., 2004; Young and Newgreen, 2001). This difference may have arisen because of the very different pattern of migration of ENS precursors along the zebrafish gut when compared with mouse and avian precursors. In zebrafish ENS, precursors initially migrate along the length of the gut tube as two symmetric streams either side of the gut mesendoderm (Elworthy et al., 2005; Shepherd et al., 2004), rather than as a

rostrocaudal cork screw wave of migration within in the gut mesoderm, as seen in mouse (Kapur et al., 1992; Young et al., 2004) and avian embryos (Burns and Douarin, 1998; Epstein et al., 1991; Newgreen et al., 1996).

An important unresolved issue is what the cellular mechanisms are that cause the ENS proliferation defect in *lsn*. One possibility is that Trap100 is required for transcription of genes that are directly involved in the cell cycle within the ENS precursors. Consistent with this idea, one of the other components of the TRAP/mediator complex is Cyclin C (Akoulitchev et al., 2000; Gu et al., 1999; Hengartner et al., 1998) and thus a mutation in Trap100 that perturbed the normal association of Cyclin C with the TRAP/mediator complex might potentially alter the effects of Cyclin C on the cell cycle (Ren and Rollins, 2004). However, this proposed mechanism assumes that the mutation acts cell autonomously within the ENS precursors. As Trap100 is not expressed in ENS precursors in the intestine (Fig. 7H,I), this cell autonomous function appears unlikely. Instead the expression of *trap100* within the intestinal endoderm suggests that the ENS defect is a secondary affect of the mutation and that the *lsn* mutation acts cell autonomously in the intestinal endoderm. Potentially the *lsn* ENS phenotype could result from reduced levels of endoderm derived mitogenic factors required by the ENS precursors. Consistent with this hypothesis is our data that shows that a lack of endoderm results in a complete loss of the ENS. Further indirect support is provided by the transplantation studies that show that the *lsn* mutation acts cell autonomously with respect to the endoderm in the pharyngeal arches. We have not been able to test this hypothesis directly as we have been unable to generate chimaeric mutant embryos that have intestinal endoderm derived principally from wild-type cells. While transplanted blastomeres from *tar**-injected donor embryos do contribute to pharyngeal pouch endoderm these transplanted cells rarely contribute to the intestinal endoderm as has been previously reported (Piotrowski et al., 2003).

A further question that also remains unanswered relates to whether the *lsn* mutant phenotype results from perturbation of nuclear hormone signalling. Previous in vitro studies have shown that Trap100 is involved in enhancing transactivation of thyroid hormone receptor (TR) and vitamin D receptor (VDR) signalling in a ligand-dependent manner (Zhang and Fondell, 1999), and that in Trap100-deficient cells TR α , VDR, PPAR γ and androgen receptors have attenuated transactivation function (Ito et al., 2002). Pharmacological block of TR signalling in zebrafish embryos between 3 dpf and 5 dpf results in a phenotype that is very similar to that seen in *lsn* mutant embryos with regard to the jaw, eye and intestinal epithelium phenotype (Liu and Chan, 2002). This study also showed by RT-PCR that both TR α and TR β are expressed in a developmentally regulated fashion during this period; however, the tissue-specific expression pattern of the receptors at this embryonic stage of development has not been described. Detailed studies investigating the precise spatial and temporal expression pattern of the thyroid hormone receptors and other nuclear hormone receptors will help determine which nuclear hormone activity is potentially perturbed in the *lsn* mutants.

In summary, the identification of *trap100* as the gene responsible for the *lsn* mutation has revealed a previously unappreciated tissue-specific function of this gene during development. This finding is of significant interest for studies relating to the function of TRAP/mediator complexes with different subunit compositions. Furthermore, the identification of Trap100 as having an important role in ENS development has potentially identified a new gene that may be associated with HSCR.

We thank Michael Pack for *foxa2* and *gata6* in situ probes; Cecilia Moens for the *rag1*, *epha4* and *hoxb4* in situ probe; Nancy Manley for the *foxn1* in situ probe; Didier Stainer for the *foxa3* in situ probe. We thank Karen Guillemain for information about the 5-HT antibody. We also thank Nancy L'Hernault for her technical assistance with the histological sectioning, Peter Kelly for technical assistance with mapping, and Thomas Schilling for his advice with the chimaeric analysis. Research was supported by grants from NIH (DK067285) and March of Dimes (5-FY02-270) to I.T.S., NIH to D.W.R., and NIH (RR12349) to W.S.T.

Supplementary material

Supplementary material for this article is available at <http://dev.biologists.org/cgi/content/full/133/3/395/DC1>

References

- Ajiro, K., Yoda, K., Utsumi, K. and Nishikawa, Y. (1996). Alteration of cell cycle-dependent histone phosphorylations by okadaic acid. Induction of mitosis-specific H3 phosphorylation and chromatin condensation in mammalian interphase cells. *J. Biol. Chem.* **271**, 13197-13201.
- Akimenko, M. A., Ekker, M., Wegner, J., Lin, W. and Westerfield, M. (1994). Combinatorial expression of three zebrafish genes related to distal-less: part of a homeobox gene code for the head. *J. Neurosci.* **14**, 3475-3486.
- Akoulitchev, S., Chuikov, S. and Reinberg, D. (2000). TFIIH is negatively regulated by cdk8-containing mediator complexes. *Nature* **407**, 102-106.
- Alexander, J., Rothenberg, M., Henry, G. L. and Stainier, D. Y. (1999). *casanova* plays an early and essential role in endoderm formation in zebrafish. *Dev. Biol.* **215**, 343-357.
- Amiel, J. and Lyonnet, S. (2001). Hirschsprung disease, associated syndromes, and genetics: a review. *J. Med. Genet.* **38**, 729-739.
- Andre, M., Ando, S., Ballagny, C., Durliat, M., Poupard, G., Briancon, C. and Babin, P. J. (2000). Intestinal fatty acid binding protein gene expression reveals the cephalocaudal patterning during zebrafish gut morphogenesis. *Int. J. Dev. Biol.* **44**, 249-252.
- Barrallo-Gimeno, A., Holzschuh, J., Driever, W. and Knapik, E. W. (2004). Neural crest survival and differentiation in zebrafish depends on *mont blanc/tap2a* gene function. *Development* **131**, 1463-1477.
- Baynash, A. G., Hosoda, K., Giaid, A., Richardson, J. A., Emoto, N., Hammer, R. E. and Yanagisawa, M. (1994). Interaction of endothelin-3 with endothelin-B receptor is essential for development of epidermal melanocytes and enteric neurons. *Cell* **79**, 1277-1285.
- Berti, L., Mittler, G., Przemec, G. K., Stelzer, G., Gunzler, B., Amati, F., Conti, E., Dallapiccola, B., Hrabe de Angelis, M., Novelli, G. et al. (2001). Isolation and characterization of a novel gene from the DiGeorge chromosomal region that encodes for a mediator subunit. *Genomics* **74**, 320-332.
- Bisgrove, B. W., Raible, D. W., Walter, V., Eisen, J. S. and Grunwald, D. J. (1997). Expression of *c-ret* in the zebrafish embryo: potential roles in motoneuronal development. *J. Neurobiol.* **33**, 749-768.
- Burns, A. J. and Douarin, N. M. (1998). The sacral neural crest contributes neurons and glia to the post-umbilical gut: spatiotemporal analysis of the development of the enteric nervous system. *Development* **125**, 4335-4347.
- Cacalano, G., Farinas, I., Wang, L. C., Hagler, K., Forgie, A., Moore, M., Armanini, M., Phillips, H., Ryan, A. M., Reichardt, L. F. et al. (1998). GFR α 1 is an essential receptor component for GDNF in the developing nervous system and kidney. *Neuron* **21**, 53-62.
- Chalazonitis, A., Rothman, T. P., Chen, J., Lamballe, F., Barbacid, M. and Gershon, M. D. (1994). Neurotrophin-3 induces neural crest-derived cells from fetal rat gut to develop in vitro as neurons or glia. *J. Neurosci.* **14**, 6571-6584.
- Chalazonitis, A., Rothman, T. P., Chen, J., Vinson, E. N., MacLennan, A. J. and Gershon, M. D. (1998). Promotion of the development of enteric neurons and glia by neurotrophic cytokines: interactions with neurotrophin-3. *Dev. Biol.* **198**, 343-365.
- Chalazonitis, A., Pham, T. D., Rothman, T. P., DiStefano, P. S., Bothwell, M., Blair-Flynn, J., Tessarollo, L. and Gershon, M. D. (2001). Neurotrophin-3 is required for the survival-differentiation of subsets of developing enteric neurons. *J. Neurosci.* **21**, 5620-5636.
- Chalazonitis, A., D'Autreaux, F., Guha, U., Pham, T. D., Faure, C., Chen, J. J., Roman, D., Kan, L., Rothman, T. P., Kessler, J. A. et al. (2004). Bone morphogenetic protein-2 and -4 limit the number of enteric neurons but promote development of a TrkC-expressing neurotrophin-3-dependent subset. *J. Neurosci.* **24**, 4266-4282.
- Concordet, J. P., Lewis, K. E., Moore, J. W., Goodrich, L. V., Johnson, R. L., Scott, M. P. and Ingham, P. W. (1996). Spatial regulation of a zebrafish patched homologue reflects the roles of sonic hedgehog and protein kinase A in neural tube and somite patterning. *Development* **122**, 2835-2846.
- Couly, G., Creuzet, S., Bennaceur, S., Vincent, C. and Le Douarin, N. M. (2002). Interactions between Hox-negative cephalic neural crest cells and the foregut endoderm in patterning the facial skeleton in the vertebrate head. *Development* **129**, 1061-1073.
- Crump, J. G., Maves, L., Lawson, N. D., Weinstein, B. M. and Kimmel, C. B.

- (2004a). An essential role for Fgfs in endodermal pouch formation influences later craniofacial skeletal patterning. *Development* **131**, 5703-5716.
- Crump, J. G., Swartz, M. E. and Kimmel, C. B.** (2004b). An integrin-dependent role of pouch endoderm in hyoid cartilage development. *PLoS Biol.* **2**, E244.
- Cserjesi, P., Brown, D., Ligon, K. L., Lyons, G. E., Copeland, N. G., Gilbert, D. J., Jenkins, N. A. and Olson, E. N.** (1995). Scleraxis: a basic helix-loop-helix protein that prefigures skeletal formation during mouse embryogenesis. *Development* **121**, 1099-1110.
- David, N. B. and Rosa, F. M.** (2001). Cell autonomous commitment to an endodermal fate and behaviour by activation of Nodal signalling. *Development* **128**, 3937-3947.
- David, N. B., Saint-Etienne, L., Tsang, M., Schilling, T. F. and Rosa, F. M.** (2002). Requirement for endoderm and FGF3 in ventral head skeleton formation. *Development* **129**, 4457-4468.
- Dickmeis, T., Mourrain, P., Saint-Etienne, L., Fischer, N., Aanstad, P., Clark, M., Strahle, U. and Rosa, F.** (2001). A crucial component of the endoderm formation pathway, CASANOVA, is encoded by a novel sox-related gene. *Genes Dev.* **15**, 1487-1492.
- Dutton, K. A., Pauliny, A., Lopes, S. S., Elworthy, S., Carney, T. J., Rauch, J., Geisler, R., Haffter, P. and Kelsh, R. N.** (2001). Zebrafish colourless encodes sox10 and specifies non-ectomesenchymal neural crest fates. *Development* **128**, 4113-4125.
- Ekker, S. C., Ungar, A. R., Greenstein, P., von Kessler, D. P., Porter, J. A., Moon, R. T. and Beachy, P. A.** (1995). Patterning activities of vertebrate hedgehog proteins in the developing eye and brain. *Curr. Biol.* **5**, 944-955.
- Elworthy, S., Pinto, J. P., Pettifer, A., Cancela, M. L. and Kelsh, R. N.** (2005). Phox2b function in the enteric nervous system is conserved in zebrafish and is sox10-dependent. *Mech. Dev.* **122**, 659-669.
- Enomoto, H., Araki, T., Jackman, A., Heuckerth, R. O., Snider, W. D., Johnson, E. M., Jr and Milbrandt, J.** (1998). GFR alpha1-deficient mice have deficits in the enteric nervous system and kidneys. *Neuron* **21**, 317-324.
- Epstein, M. L., Poulsen, K. T. and Thiboldeaux, R.** (1991). Formation of ganglia in the gut of the chick embryo. *J. Comp. Neurol.* **307**, 189-199.
- Fu, M., Lui, V. C., Sham, M. H., Pachnis, V. and Tam, P. K.** (2004). Sonic hedgehog regulates the proliferation, differentiation, and migration of enteric neural crest cells in gut. *J. Cell Biol.* **166**, 673-684.
- Furness, J. B. and Costa, M.** (1987). *The Enteric Nervous System*. Glasgow: Churchill Livingstone.
- Gavrieli, Y., Sherman, Y. and Ben Sasson, S. A.** (1992). Identification of programmed cell death in situ via specific labeling of nuclear DNA fragmentation. *J. Cell Biol.* **119**, 493-501.
- Gershon, M. D., Kirchgessner, A. L. and Wade, P. R.** (1994). Functional anatomy of the enteric nervous system. In *Physiology of the Gastrointestinal Tract*, Vol. 1 (ed. L. R. Johnson). New York: Raven Press.
- Gu, W., Malik, S., Ito, M., Yuan, C. X., Fondell, J. D., Zhang, X., Martinez, E., Qin, J. and Roeder, R. G.** (1999). A novel human SRB/MED-containing cofactor complex, SMCC, involved in transcription regulation. *Mol. Cell* **3**, 97-108.
- Guillemot, F., Lo, L. C., Johnson, J. E., Auerbach, A., Anderson, D. J. and Joyner, A. L.** (1993). Mammalian achaete-scute homolog 1 is required for the early development of olfactory and autonomic neurons. *Cell* **75**, 463-476.
- Haffter, P., Granato, M., Brand, M., Mullins, M. C., Hammerschmidt, M., Kane, D. A., Odenthal, J., van Eeden, F. J., Jiang, Y. J., Heisenberg, C. P. et al.** (1996). The identification of genes with unique and essential functions in the development of the zebrafish, *Danio rerio*. *Development* **123**, 1-36.
- Hall, B. K.** (1980). Tissue interactions and the initiation of osteogenesis and chondrogenesis in the neural crest-derived mandibular skeleton of the embryonic mouse as seen in isolated murine tissues and in recombinations of murine and avian tissues. *J. Embryol. Exp. Morphol.* **58**, 251-264.
- Hatano, M., Aoki, T., Dezawa, M., Yusa, S., Iitsuka, Y., Koseki, H., Taniguchi, M. and Tokuhisa, T.** (1997). A novel pathogenesis of megacolon in *Ncx/Hox11L.1* deficient mice. *J. Clin. Invest.* **100**, 795-801.
- Hengartner, C. J., Myer, V. E., Liao, S. M., Wilson, C. J., Koh, S. S. and Young, R. A.** (1998). Temporal regulation of RNA polymerase II by *Srb10* and *Kin28* cyclin-dependent kinases. *Mol. Cell* **2**, 43-53.
- Herbarth, B., Pingault, V., Bondurand, N., Kuhlbrodt, K., Hermans Borgmeyer, I., Puliti, A., Lemort, N., Goossens, M. and Wegner, M.** (1998). Mutation of the Sry-related *Sox10* gene in Dominant megacolon, a mouse model for human Hirschsprung disease. *Proc. Natl. Acad. Sci. USA.* **95**, 5161-5165.
- Heuckerth, R. O., Lampe, P. A., Johnson, E. M. and Milbrandt, J.** (1998). Neurturin and GDNF promote proliferation and survival of enteric neuron and glial progenitors in vitro. *Dev. Biol.* **200**, 116-129.
- Heuckerth, R. O., Enomoto, H., Gridler, J. R., Golden, J. P., Hanke, J. A., Jackman, A., Molliver, D. C., Bardgett, M. E., Snider, W. D., Johnson, E. M., Jr et al.** (1999). Gene targeting reveals a critical role for neurturin in the development and maintenance of enteric, sensory, and parasympathetic neurons. *Neuron* **22**, 253-263.
- Holzschuh, J., Wada, N., Wada, C., Schaffer, A., Javidan, Y., Tallafuss, A., Bally-Cuif, L. and Schilling, T. F.** (2005). Requirements for endoderm and BMP signalling in sensory neurogenesis in zebrafish. *Development* **132**, 3731-3742.
- Hosoda, K., Hammer, R. E., Richardson, J. A., Baynash, A. G., Cheung, J. C., Gaid, A. and Yanagisawa, M.** (1994). Targeted and natural (piebald-lethal) mutations of endothelin-B receptor gene produce megacolon associated with spotted coat color in mice. *Cell* **79**, 1267-1276.
- Howard, M., Foster, D. N. and Cserjesi, P.** (1999). Expression of HAND gene products may be sufficient for the differentiation of avian neural crest-derived cells into catecholaminergic neurons in culture. *Dev. Biol.* **215**, 62-77.
- Ito, M., Yuan, C. X., Okano, H. J., Darnell, R. B. and Roeder, R. G.** (2000). Involvement of the TRAP220 component of the TRAP/SMCC coactivator complex in embryonic development and thyroid hormone action. *Mol. Cell* **5**, 683-693.
- Ito, M., Okano, H. J., Darnell, R. B. and Roeder, R. G.** (2002). The TRAP100 component of the TRAP/Mediator complex is essential in broad transcriptional events and development. *EMBO J.* **21**, 3464-3475.
- Jerome, L. A. and Papaioannou, V. E.** (2001). DiGeorge syndrome phenotype in mice mutant for the T-box gene, *Tbx1*. *Nat. Genet.* **27**, 286-291.
- Kapur, R. P.** (1999a). Early death of neural crest cells is responsible for total enteric aganglionosis in *Sox10(Dom)/Sox10(Dom)* mouse embryos. *Pediatr. Dev. Pathol.* **2**, 559-569.
- Kapur, R. P.** (1999b). Hirschsprung disease and other enteric dysganglionoses. *Crit. Rev. Clin. Lab. Sci.* **36**, 225-273.
- Kapur, R. P., Yost, C. and Palmiter, R. D.** (1992). A transgenic model for studying development of the enteric nervous system in normal and aganglionic mice. *Development* **116**, 167-175.
- Kelsh, R. N. and Eisen, J. S.** (2000). The zebrafish colourless gene regulates development of non-ectomesenchymal neural crest derivatives. *Development* **127**, 515-525.
- Kikuchi, Y., Agathon, A., Alexander, J., Thisse, C., Waldron, S., Yelon, D., Thisse, B. and Stainier, D. Y.** (2001). casanova encodes a novel Sox-related protein necessary and sufficient for early endoderm formation in zebrafish. *Genes Dev.* **15**, 1493-1505.
- Kimmel, C. B., Ullmann, B., Walker, M., Miller, C. T. and Crump, J. G.** (2003). Endothelin 1-mediated regulation of pharyngeal bone development in zebrafish. *Development* **130**, 1339-1351.
- Knight, R. D., Nair, S., Nelson, S. S., Afshar, A., Javidan, Y., Geisler, R., Rauch, G. J. and Schilling, T. F.** (2003). *lockjaw* encodes a zebrafish *trap2a* required for early neural crest development. *Development* **130**, 5755-5768.
- Kuratani, S. C. and Wall, N. A.** (1992). Expression of Hox 2.1 protein in restricted populations of neural crest cells and pharyngeal ectoderm. *Dev. Dyn.* **195**, 15-28.
- Lam, S. H., Chua, H. L., Gong, Z., Wen, Z., Lam, T. J. and Sin, Y. M.** (2002). Morphologic transformation of the thymus in developing zebrafish. *Dev. Dyn.* **225**, 87-94.
- Lewis, K. E., Concordet, J. P. and Ingham, P. W.** (1999). Characterisation of a second patched gene in the zebrafish *Danio rerio* and the differential response of patched genes to Hedgehog signalling. *Dev. Biol.* **208**, 14-29.
- Lindsay, E. A., Vitelli, F., Su, H., Morishima, M., Huynh, T., Pramparo, T., Jurecic, V., Ogunrinu, G., Sutherland, H. F., Scambler, P. J. et al.** (2001). *Tbx1* haploinsufficiency in the DiGeorge syndrome region causes aortic arch defects in mice. *Nature* **410**, 97-101.
- Lister, J. A., Robertson, C. P., Lepage, T., Johnson, S. L. and Raible, D. W.** (1999). *nacre* encodes a zebrafish microphthalmia-related protein that regulates neural-crest-derived pigment cell fate. *Development* **126**, 3757-3767.
- Liu, Y. W. and Chan, W. K.** (2002). Thyroid hormones are important for embryonic to larval transitory phase in zebrafish. *Differentiation* **70**, 36-45.
- Luo, R., An, M., Arduini, B. L. and Henion, P. D.** (2001). Specific pan-neural crest expression of zebrafish *Crestin* throughout embryonic development. *Dev. Dyn.* **220**, 169-174.
- Malik, S. and Roeder, R. G.** (2000). Transcriptional regulation through Mediator-like coactivators in yeast and metazoan cells. *Trends Biochem. Sci.* **25**, 277-283.
- Marusch, M. F., Furneaux, H. M., Henion, P. D. and Weston, J. A.** (1994). Hu neuronal proteins are expressed in proliferating neurogenic cells. *J. Neurobiol.* **25**, 143-155.
- Mayer, A. N. and Fishman, M. C.** (2003). *Nil per os* encodes a conserved RNA recognition motif protein required for morphogenesis and cytodifferentiation of digestive organs in zebrafish. *Development* **130**, 3917-3928.
- Merscher, S., Funke, B., Epstein, J. A., Heyer, J., Puech, A., Lu, M. M., Xavier, R. J., Demay, M. B., Russell, R. G., Factor, S. et al.** (2001). *TBX1* is responsible for cardiovascular defects in velo-cardio-facial/DiGeorge syndrome. *Cell* **104**, 619-629.
- Miller, C. T., Schilling, T. F., Lee, K., Parker, J. and Kimmel, C. B.** (2000). *sucker* encodes a zebrafish Endothelin-1 required for ventral pharyngeal arch development. *Development* **127**, 3815-3828.
- Moore, M. W., Klein, R. D., Farinas, I., Sauer, H., Armanini, M., Phillips, H., Reichardt, L. F., Ryan, A. M., Carver-Moore, K. and Rosenthal, A.** (1996). Renal and neuronal abnormalities in mice lacking GDNF. *Nature* **382**, 76-79.
- Myers, L. C. and Kornberg, R. D.** (2000). Mediator of transcriptional regulation. *Annu. Rev. Biochem.* **69**, 729-749.
- Nechiporuk, A., Linbo, T. and Raible, D. W.** (2005). Endoderm-derived *Fgf3* is necessary and sufficient for inducing neurogenesis in the epibranchial placodes in zebrafish. *Development* **132**, 3717-3730.

- Newgreen, D. and Young, H. M. (2002a). Enteric nervous system: development and developmental disturbances – part 1. *Pediatr. Dev. Pathol.* **5**, 224-247.
- Newgreen, D. and Young, H. M. (2002b). Enteric nervous system: development and developmental disturbances – part 2. *Pediatr. Dev. Pathol.* **5**, 329-349.
- Newgreen, D. F., Southwell, B., Hartley, L. and Allan, I. J. (1996). Migration of enteric neural crest cells in relation to growth of the gut in avian embryos. *Acta Anat. (Basel)* **157**, 105-115.
- Ng, A. N., de Jong-Curtain, T. A., Mawdsley, D. J., White, S. J., Shin, J., Appel, B., Dong, P. D., Stainier, D. Y. and Heath, J. K. (2005). Formation of the digestive system in zebrafish: III. Intestinal epithelium morphogenesis. *Dev. Biol.* **286**, 114-135.
- Nornes, S., Mikkola, I., Krauss, S., Delghandi, M., Perander, M. and Johansen, T. (1996). Zebrafish Pax9 encodes two proteins with distinct C-terminal transactivating domains of different potency negatively regulated by adjacent N-terminal sequences. *J. Biol. Chem.* **271**, 26914-26923.
- O'Brien, E. K., d'Alencon, C., Bonde, G., Li, W., Schoenebeck, J., Allende, M. L., Gelb, B. D., Yelon, D., Eisen, J. S. and Cornell, R. A. (2004). Transcription factor Ap-2alpha is necessary for development of embryonic melanophores, autonomic neurons and pharyngeal skeleton in zebrafish. *Dev. Biol.* **265**, 246-261.
- Odenthal, J. and Nusslein-Volhard, C. (1998). fork head domain genes in zebrafish. *Dev. Genes Evol.* **208**, 245-258.
- Pack, M., Solnica-Krezel, L., Malicki, J., Neuhauss, S. C., Schier, A. F., Stemple, D. L., Driever, W. and Fishman, M. C. (1996). Mutations affecting development of zebrafish digestive organs. *Development* **123**, 321-328.
- Pattyn, A., Morin, X., Cremer, H., Goridis, C. and Brunet, J. F. (1997). Expression and interactions of the two closely related homeobox genes Phox2a and Phox2b during neurogenesis. *Development* **124**, 4065-4075.
- Pattyn, A., Morin, X., Cremer, H., Goridis, C. and Brunet, J. F. (1999). The homeobox gene Phox2b is essential for the development of autonomic neural crest derivatives. *Nature* **399**, 366-370.
- Peyrieras, N., Strahle, U. and Rosa, F. (1998). Conversion of zebrafish blastomeres to an endodermal fate by TGF-beta-related signaling. *Curr. Biol.* **8**, 783-786.
- Pichel, J. G., Shen, L., Sheng, H. Z., Granholm, A. C., Drago, J., Grinberg, A., Lee, E. J., Huang, S. P., Saarma, M., Hoffer, B. J. et al. (1996). Defects in enteric innervation and kidney development in mice lacking GDNF. *Nature* **382**, 73-76.
- Piotrowski, T., Ahn, D. G., Schilling, T. F., Nair, S., Ruvinsky, I., Geisler, R., Rauch, G. J., Haffter, P., Zon, L. I., Zhou, Y. et al. (2003). The zebrafish van gogh mutation disrupts *tbx1*, which is involved in the DiGeorge deletion syndrome in humans. *Development* **130**, 5043-5052.
- Pitera, J. E., Smith, V. V., Thorogood, P. and Milla, P. J. (1999). Coordinated expression of 3' *hox* genes during murine embryonic gut development: an enteric Hox code. *Gastroenterology* **117**, 1339-1351.
- Poon, K. L., Richardson, M., Lam, C. S., Khoo, H. E. and Korzh, V. (2003). Expression pattern of neuronal nitric oxide synthase in embryonic zebrafish. *Gene Expr. Patterns* **3**, 463-466.
- Prince, V. E., Moens, C. B., Kimmel, C. B. and Ho, R. K. (1998). Zebrafish *hox* genes: expression in the hindbrain region of wild-type and mutants of the segmentation gene, *valentino*. *Development* **125**, 393-406.
- Puri, P., Ohshiro, K. and Wester, T. (1998). Hirschsprung's disease: a search for etiology. *Semin. Pediatr. Surg.* **7**, 140-147.
- Rachez, C. and Freedman, L. P. (2001). Mediator complexes and transcription. *Curr. Opin. Cell Biol.* **13**, 274-280.
- Raible, D. W. and Kruse, G. J. (2000). Organization of the lateral line system in embryonic zebrafish. *J. Comp. Neurol.* **421**, 189-198.
- Ramalho-Santos, M., Melton, D. A. and McMahon, A. P. (2000). Hedgehog signals regulate multiple aspects of gastrointestinal development. *Development* **127**, 2763-2772.
- Ren, S. and Rollins, B. J. (2004). Cyclin C/*cdk3* promotes Rb-dependent G0 exit. *Cell* **117**, 239-251.
- Rossi, J., Luukko, K., Poteryaev, D., Laurikainen, A., Sun, Y. F., Laakso, T., Eerikainen, S., Tuominen, R., Lakso, M., Rauvala, H. et al. (1999). Retarded growth and deficits in the enteric and parasympathetic nervous system in mice lacking GFR alpha2, a functional neurturin receptor. *Neuron* **22**, 243-252.
- Roy, S., Qiao, T., Wolff, C. and Ingham, P. W. (2001). Hedgehog signaling pathway is essential for pancreas specification in the zebrafish embryo. *Curr. Biol.* **11**, 1358-1363.
- Rubinstein, A. L., Lee, D., Luo, R., Henion, P. D. and Halpern, M. E. (2000). Genes dependent on zebrafish *cyclops* function identified by APLP differential gene expression screen. *Genesis* **26**, 86-97.
- Schilling, T. F. and Kimmel, C. B. (1994). Segment and cell type lineage restrictions during pharyngeal arch development in the zebrafish embryo. *Development* **120**, 483-494.
- Schilling, T. F., Piotrowski, T., Grandel, H., Brand, M., Heisenberg, C. P., Jiang, Y. J., Beuchle, D., Hammerschmidt, M., Kane, D. A., Mullins, M. C. et al. (1996). Jaw and branchial arch mutants in zebrafish I: branchial arches. *Development* **123**, 329-344.
- Schorpp, M., Leicht, M., Nold, E., Hammerschmidt, M., Haas-Assenbaum, A., Wiest, W. and Boehm, T. (2002). A zebrafish orthologue (*whnb*) of the mouse nude gene is expressed in the epithelial compartment of the embryonic thymic rudiment. *Mech. Dev.* **118**, 179-185.
- Schuchardt, A., D'Agati, V., Larsson-Blomberg, L., Costantini, F. and Pachnis, V. (1994). Defects in the kidney and enteric nervous system of mice lacking the tyrosine kinase receptor Ret. *Nature* **367**, 380-383.
- Shepherd, I. T., Beattie, C. E. and Raible, D. W. (2001). Functional analysis of zebrafish GDNF. *Dev. Biol.* **231**, 420-435.
- Shepherd, I. T., Pietsch, J., Elworthy, S., Kelsh, R. N. and Raible, D. W. (2004). Roles for GFR[alpha]1 receptors in zebrafish enteric nervous system development. *Development* **131**, 241-249.
- Shimoda, N., Knapik, E. W., Ziniti, J., Sim, C., Yamada, E., Kaplan, S., Jackson, D., de Sauvage, F., Jacob, H. and Fishman, M. C. (1999). Zebrafish genetic map with 2000 microsatellite markers. *Genomics* **58**, 219-232.
- Shirasawa, S., Yunker, A. M., Roth, K. A., Brown, G. A., Horning, S. and Korsmeyer, S. J. (1997). Enx (Hox11L1)-deficient mice develop myenteric neuronal hyperplasia and megacolon. *Nat. Med.* **3**, 646-650.
- Southard Smith, E. M., Kos, L. and Pavan, W. J. (1998). Sox10 mutation disrupts neural crest development in Dom Hirschsprung mouse model. *Nat. Genet.* **18**, 60-64.
- Srivastava, D., Cserjesi, P. and Olson, E. N. (1995). A subclass of bHLH proteins required for cardiac morphogenesis. *Science* **270**, 1995-1999.
- Stickney, H. L., Schmutz, J., Woods, I. G., Holtzer, C. C., Dickson, M. C., Kelly, P. D., Myers, R. M. and Talbot, W. S. (2002). Rapid mapping of zebrafish mutations with SNPs and oligonucleotide microarrays. *Genome Res.* **12**, 1929-1934.
- Strahle, U., Blader, P., Henrique, D. and Ingham, P. W. (1993). Axial, a zebrafish gene expressed along the developing body axis, shows altered expression in *cyclops* mutant embryos. *Genes Dev.* **7**, 1436-1446.
- Sukegawa, A., Narita, T., Kameda, T., Saitoh, K., Nohno, T., Iba, H., Yasugi, S. and Fukuda, K. (2000). The concentric structure of the developing gut is regulated by Sonic hedgehog derived from endodermal epithelium. *Development* **127**, 1971-1980.
- Talbot, W. S. and Schier, A. F. (1999). Positional cloning of mutated zebrafish genes. *Methods Cell Biol.* **60**, 259-286.
- Thisse, C., Thisse, B., Schilling, T. F. and Postlethwait, J. H. (1993). Structure of the zebrafish *snail1* gene and its expression in wild-type, spadetail and no tail mutant embryos. *Development* **119**, 1203-1215.
- Tudor, M., Murray, P. J., Onufryk, C., Jaenisch, R. and Young, R. A. (1999). Ubiquitous expression and embryonic requirement for RNA polymerase II coactivator subunit *Srb7* in mice. *Genes Dev.* **13**, 2365-2368.
- Westerfield, M. (1993). *The Zebrafish Book*. Eugene (OR): University of Oregon Press.
- Willett, C. E., Zapata, A. G., Hopkins, N. and Steiner, L. A. (1997). Expression of zebrafish *rag* genes during early development identifies the thymus. *Dev. Biol.* **182**, 331-341.
- Wu, X. and Howard, M. J. (2002). Transcripts encoding HAND genes are differentially expressed and regulated by BMP4 and GDNF in developing avian gut. *Gene Expr.* **10**, 279-293.
- Xu, Q., Alldus, G., Holder, N. and Wilkinson, D. G. (1995). Expression of truncated Sek-1 receptor tyrosine kinase disrupts the segmental restriction of gene expression in the *Xenopus* and zebrafish hindbrain. *Development* **121**, 4005-4016.
- Yanagisawa, H., Yanagisawa, M., Kapur, R. P., Richardson, J. A., Williams, S. C., Clouthier, D. E., de Wit, D., Emoto, N. and Hammer, R. E. (1998). Dual genetic pathways of endothelin-mediated intercellular signaling revealed by targeted disruption of endothelin converting enzyme-1 gene. *Development* **125**, 825-836.
- Yelick, P. C. and Schilling, T. F. (2002). Molecular dissection of craniofacial development using zebrafish. *Crit. Rev. Oral Biol. Med.* **13**, 308-322.
- Young, H. M. and Newgreen, D. (2001). Enteric neural crest-derived cells: origin, identification, migration, and differentiation. *Anat. Rec.* **262**, 1-15.
- Young, H. M., Bergner, A. J., Anderson, R. B., Enomoto, H., Milbrandt, J., Newgreen, D. F. and Whittington, P. M. (2004). Dynamics of neural crest-derived cell migration in the embryonic mouse gut. *Dev. Biol.* **270**, 455-473.
- Yuan, C. X., Ito, M., Fondell, J. D., Fu, Z. Y. and Roeder, R. G. (1998). The TRAP220 component of a thyroid hormone receptor-associated protein (TRAP) coactivator complex interacts directly with nuclear receptors in a ligand-dependent fashion. *Proc. Natl. Acad. Sci. USA* **95**, 7939-7944.
- Zhang, J. and Fondell, J. D. (1999). Identification of mouse TRAP100: a transcriptional coregulatory factor for thyroid hormone and vitamin D receptors. *Mol. Endocrinol.* **13**, 1130-1140.
- Zhu, Y., Qi, C., Jia, Y., Nye, J. S., Rao, M. S. and Reddy, J. K. (2000). Deletion of PBP/PPARBP, the gene for nuclear receptor coactivator peroxisome proliferator-activated receptor-binding protein, results in embryonic lethality. *J. Biol. Chem.* **275**, 14779-14782.